Nuclear Inst, and Methods in Physics Research B 431 (2018) 59–66

Contents lists available at ScienceDirect

Nuclear Inst. and Methods in Physics Research B

journal homepage: www.elsevier.com/locate/nimb

Enhancing the extraction of laser-ionized beams from an arc discharge ion source volume

Y. Martinez Palenzuela[a,c,*], B.A. Marsh[a], J. Ballof[a,b], R. Catherall[a], K. Chrysalidis[a,d], T.E. Cocolios[c], B. Crepieux[a], T. Day Goodacre[a,e,f], V.N. Fedosseev[a], M.H. Huyse[c], P.B. Larmonier[a,g], J.P. Ramos[a], S. Rothe[a], J.D.A. Smith[h], T. Stora[a], P. Van Duppen[c], S. Wilkins[a]

[a] CERN, CH-1211 Geneva 23, Switzerland
[b] Institut für Kernchemie, Johannes Gutenberg Universität, D-55099 Mainz, Germany
[c] KU Leuven, Instituut voor Kern- en Stralingsfysica, B-3001 Leuven, Belgium
[d] Institut für Physik, Johannes Gutenberg Universität, D-55099 Mainz, Germany
[e] School of Physics and Astronomy, The University of Manchester, Manchester M13 9PL, United Kingdom
[f] TRIUMF, 4004 Wesbrook Mall, Vancouver, BC V6T 2A3, Canada
[g] Ministère des Affaires Étrangères et Européennes, 37 Quai d'Orsay, 75007 Paris, France
[h] Tech-X UK Ltd, Sci-Tech Daresbury, Warrington, UK

ARTICLE INFO

Keywords:
Ion source
Resonance laser ionization
Arc discharge ionization
Radioactive ion beams
Particle-in-cell simulation

ABSTRACT

The Versatile Arc Discharge and Laser Ion Source (VADLIS) is a recently established ion source for the CERN-ISOLDE radioactive ion beam facility. It offers either electron-impact ionization (VADIS-mode) or resonance laser ionization (RILIS-mode). The choice of operating mode depends on the element of interest or the required beam purity. Particle-in-cell simulations using the VSim software show that the ion extraction efficiency of the VADLIS in RILIS-mode can be improved if it is equipped with an insulated extractor plate, to which an optimal voltage can be applied. This enables optimization of the RILIS-mode ion extraction independently of the electron density. Experiments have been performed using a prototype VADLIS with an adjustable extractor plate voltage for the generation of gallium ion beams at the off-line separator as well as magnesium, molybdenum and mercury ion beams at ISOLDE. A factor > 2 increase of the VADLIS efficiency in RILIS-mode has been achieved.

1. Introduction

The Versatile Arc Discharge and Laser Ion Source [1] (VADLIS) combines the FEBIAD (Forced Electron Beam Induced Arc Discharge) ion source [2] and the RILIS (Resonance Ionization Laser Ion Source) [3], both employed at Isotope Separator On Line (ISOL) facilities for the production of radioactive ion beams. The ISOLDE variant of the FEBIAD is known as the VADIS (Versatile Arc Discharge Ion Source) [4] but they share the same design and operating principle based on electron impact ionization. At ISOLDE [5], reaction products (radioactive isotopes) produced in the high-temperature target effuse as atomic vapor towards the anode volume of the ion source, via a transfer line. The transfer line is connected to the cathode tube (see Fig. 1) through which the atoms effuse into the anode cavity, where they are ionized, primarily by electron bombardment. Electrons are emitted by thermionic emission from the flat surface of the cathode which is resistively heated to typically 2000 °C. A positive voltage is applied to the anode cavity (typically in the range of 100 V to 150 V). Electrons are therefore accelerated towards the grid. Those that pass into the anode do so as a mono-energetic electron beam with an energy corresponding to the anode voltage. An axial magnetic field, regulated by the current applied to the coils of a fixed solenoid installed around the ion source volume, increases the mean path length of the electron trajectory thus increasing the probability of an electron/atom interaction. The VADIS series of ion sources all use the anode geometry of the MK5 FEBIAD [6] though the material of the grid was replaced from graphite to molybdenum in an effort to reduce the CO^+ ion formation. The total ion load of the cavity decreases creating a low density plasma [4]. Previous experimental studies indicate a complex relationship between the anode voltage (electron energy) and the overall ion source performance [4]:

- The electron energy must exceed the ionization potential of the element of interest. The ionization cross section varies with electron energy and peaks at a value typically equal to 2–3 times the ionization potential.
- If the electron emission from the cathode is space-charge limited,

* Corresponding author.
E-mail address: yisel.martinez@cern.ch (Y. Martinez Palenzuela).

https://doi.org/10.1016/j.nimb.2018.06.006
Received 3 April 2018; Received in revised form 6 June 2018; Accepted 8 June 2018

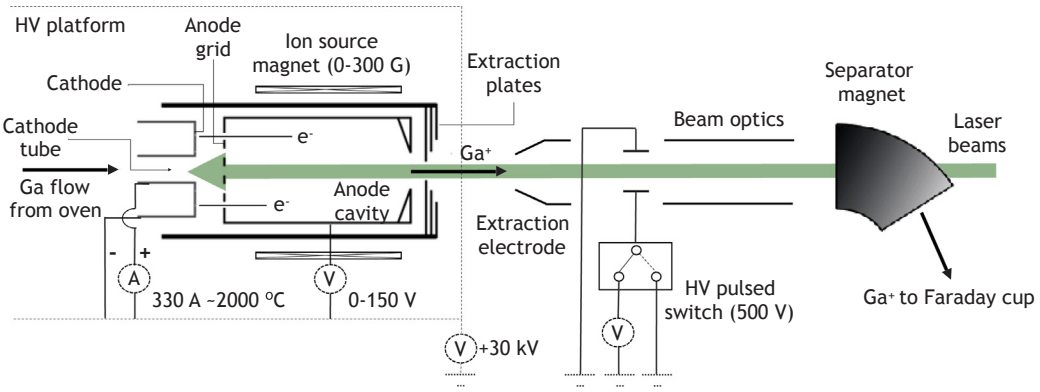

Fig. 1. Sketch of the VADLIS and general description of the experimental set-up. (not to scale).

then the electron flux is proportional to $V^{\frac{3}{2}}/d^2$, where V is the voltage difference and d the distance between the cathode and the anode [7].

- The anode body temperature is determined by its proximity to the hot cathode (~2000 °C). The anode is also heated by electron bombardment, which is determined by the electron current and the anode voltage. The anode temperature influences the surface ionization rate of the atoms and wall sticking times as well as electron emission from the walls. Theoretical estimations are given in [8].
- For the standard VADIS configuration, the extraction plates are held at the potential of the high voltage platform as indicated in Fig. 1 (locally grounded). The voltage difference between the anode and extraction plates is therefore equivalent to the anode voltage.

It is challenging to experimentally determine the relative importance of each of these aspects of the ion source in terms of the resulting ionization efficiency for a given species. For this reason, particle-in-cell (PIC) simulations of the ion source, for which individual physical effects can be switched on and off, can therefore provide a valuable insight. The CPO software [9] has been used in the past to demonstrate the impact of the so called 'active' volume in the overall efficiency of the ion source. A model describing the dependance between efficiency and the active volume was then inferred from experimental results over a wide range of operational parameters. More details can be found in [4,10].

Recently it was demonstrated that the VADIS cavity could be used as an effective laser-atom interaction region provided that the lasers can be transmitted through the 1.5 mm diameter exit aperture of the anode [1]. In this case the ion source is operated in so-called RILIS-mode, with the source magnet and the anode voltage optimized for laser-ion survival and extraction, whilst keeping the anode voltage below the required value for electron impact ionization to occur.

The development of this multi-purpose ion source (known as the VADLIS) has been crucial to the success of several experiments at ISOLDE since its first on-line use in 2015. For example, this approach enabled the first operation of RILIS with molten lead targets for the study of mercury isotopes by in-source laser spectroscopy [11] since a reliable means of coupling the standard hot cavity RILIS ion source with liquid targets does not currently exist. On-line experiments for the production of mercury, cadmium and magnesium beams have shown that RILIS-mode achieves a beam purity comparable to that of the standard hot-cavity RILIS ion source as well as an operating efficiency comparable to VADIS-mode for the laser-ionized species [1,11]. This additional degree of ion source flexibility proved vital to the success of the ISOLTRAP [12] experiment at ISOLDE described in Ref. [13,14] for which magnesium and neon beams were required in a single experiment and thus one target/ion source assembly should be used. Beams of neon isotopes need an electron impact ionization mechanism while magnesium can be ionized by both electron impact and laser ionization (RILIS). The RILIS-mode allowed the ^{23}Mg yield to be preserved with a much cleaner isobaric spectrum compared to the VADIS-mode (electron impact ionization).

In this work we characterize the performance of a modified VADLIS, equipped with an adjustable-voltage extractor plate, primarily intended to improve the performance of the RILIS-mode of operation in terms of selectivity and extraction efficiency. This is highly desirable at ISOL facilities: e.g users would benefit from a reduced number of shifts necessary to perform their experiments without any apparent drawback. Even though the VADIS operation mode can also benefit from these modifications, the enhancement in extraction efficiency was observed to be not as significant as for the RILIS-mode. We demonstrate that the source can perform as a standard VADIS with no loss of performance or drop in lifetime. The particle-in-cell software VSim [15,16] is used to study improved RILIS-mode extraction characteristics. VSim is also used to simulate the ion extraction time profile which shows good agreement with experimental results. In the outlook we discuss the prospects of this modified VADLIS as the new standard configuration, and suggest further modifications for improved ion source flexibility, diagnostics and performance.

2. Experimental set-up

The study performed in Ref. [1], which identified the different modes of operation of the VADLIS served as a starting point for a better understanding and optimization of the anode cavity as an efficient laser-atom interaction volume. The experimental studies were carried out at the ISOLDE off-line laboratory described in Ref. [8]. Gallium vapor was released from a $GaNO_3$ precipitate contained in a resistively-heated capillary oven, connected to the rear of the tubular cathode tube. Atomic Ga (ionization potential ~6.0 eV) effusing along the cathode tube is able to enter the anode cavity by passing through the anode grid, located 1 to 2 mm downstream of the cathode exit. The Ga atoms were ionized via a two-step, one-resonance ionization scheme (294.36 nm,532 nm) [17]. The first step involves a transition from the thermally-populated low-lying atomic energy level $3d^{10}4s^24p^2P^0_{3/2}$ to the $4s^24d^2D_{5/2}$ state. Up to 200 mW of 294.36 nm light was produced using a frequency-doubled Rhodamine 6G dye laser, pumped by 20W of 532 nm radiation from a frequency-doubled Nd:YAG laser (Edgewave IS series). The second step, non-resonant ionization to the continuum made use of up to 15W of residual 532 nm light from the dye pump laser. An optical delay line ensured coincidence of the ~8ns laser pulses in the ion source. The laser pulse repetition rate was fixed to 10 kHz for these studies.

The laser beams are transmitted to the ion source through a fused silica window in the separator vacuum chamber and enter the anode volume through the 1.5 mm diameter aperture of the anode extractor plate. A portion of the laser beams passes through both the anode cavity and the central hole of the anode grid, entering the cathode tube

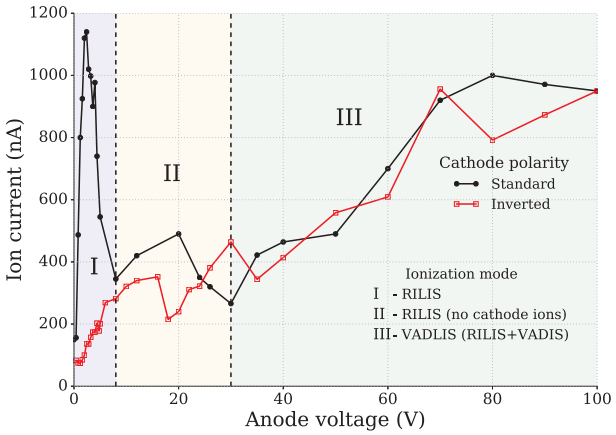

Fig. 2. Ga^+ beam intensity as a function of the anode voltage (black line). The different regions show the Ga^+ signal from ions created by the laser beams in the anode and cathode (region I, V_a ~[0, 7 V]), ions created only inside the anode (region II) and by electron impact ionization plus resonance ionization (region III). Details on the contribution of different ionization mechanisms to the Ga^+ signal are discussed in [1]. The red line represents the Ga^+ beam intensity as a function of the anode voltage when the cathode polarity is inverted (see subSection 2.1)

(diameter 1.2 mm, length 22 mm) as shown in Fig. 1. The ion source assembly is on a high voltage platform, held at +30 kV. A grounded extraction electrode, located ~60 mm downstream of the anode exit, extracts ions as a 30keV, effectively mono-energetic beam, which is transmitted through a magnetic dipole mass separator for isotope selection. After mass/charge selection the ion beam is transported to a Faraday cup as shown in Fig. 1.

The beamline is equipped with a high voltage pulsed switch (BEHLKE GHTS60) connected to a vertical deflector downstream of the extraction electrode, also shown in Fig. 1. By using a sliding beam gate technique, the time structure of the extracted beam can be obtained as discussed in Section 3.2.

The dependence of the $^{71}Ga^+$ current while sending the lasers into the anode cavity, as a function of the anode voltage V_a, is shown in Fig. 2. In the analysis of the ion source performance we assume a constant atomic Ga flux into the anode (i.e. the effect of the electron-bombardment heating of the anode on the Ga evaporation rate from the oven is negligible).

Three regions can be identified in the anode voltage scan. Below $V_a = 30$ V laser-ionization is the dominant ionization mechanism. The highest ion signal is recorded at values of V_a for which the kinetic energy of the ions created by the laser pulse within the cathode tube is sufficient to overcome the voltage of the anode grid (region I). As the anode voltage increases region II is reached. At this stage, the positive anode grid potential exceeds the potential difference along the resistively heated cathode tube (Fig. 1). Laser-ions originating from inside the cathode tube are therefore prevented from entering the anode volume and the ion current decreases. At around 30 V, electron impact ionization becomes the predominant ionization mechanism and the ion source operates in the standard VADLIS regime (region III).

2.1. Cathode with inverted polarity

The survival of ions created inside the cathode tube is expected to be enhanced by the 'hot cavity effect' [18,19]. The voltage drop along the resistively heated cathode tube acts as a drift field for any ions created in that region. The direction of ion flow depends on the polarity of the power supply. In the standard configuration, there is a negative voltage gradient towards the anode-end of the cavity, attracting positively-charged ions towards the anode. These ions can be generated either by laser or surface ionization. If the polarity of the cathode is inverted, the ion flow along the cathode towards the anode is suppressed.

Fig. 2 compares the Ga^+ ion rate (combined effect of laser, surface and electron-impact ionized) dependence on the anode voltage with standard and inverted cathode heating current polarity. The disappearance of the ion current peak in region I in the case of inverted polarity confirms our interpretation that the observed ions at low anode voltage originate from inside the hot cathode tube itself.

Alkali suppression could be achieved by equipping the target assembly with a resistively heated transfer line, with inverted polarity, between the RILIS cavity and the target as discussed in Ref. [20]. In Section 4.3 we will discuss this aspect and how the overall RILIS-mode selectivity can be increased under certain conditions by making use of the same mechanism for surface ion suppression using the cathode itself. This is possible since the MK5-type ISOLDE ion sources are capable of operation with an inverted polarity [20].

3. Particle-in-cell simulations for the characterization of the VADIS electrostatic cavity

The software VSim from Tech-X Corporation [15,16] is used in the present work to model the electrostatic field distribution within the VADIS cavity and gain an insight into the RILIS-mode ion dynamics. It contains a well validated implementation of the electrostatic particle-in-cell (PIC) algorithm with Monte Carlo treatment for the field ionization, impact ionization as well as elastic and inelastic scattering processes.

In this study we focus on the electric field distribution caused by the electrons reaching the anode cavity, combined with the voltages applied to the ion source walls and external electrostatic fields reaching the extraction zone. When the rate of electron supply to the anode (electrons incident from the cathode, plus those generated through collisions with the atoms and anode walls) matches the rate of electron absorption on the walls of the anode, a quasi-steady state is reached for the electron population and, accordingly for the electric field distribution. The electron current extracted from the cathode and injected into the anode volume in VADIS-mode is of the order of some tens of mA while the typical ion current extracted from the anode volume through the exit aperture reaches at maximum several μA. We therefore consider in the present study that the ion density inside the anode volume has a negligible influence on the quasi-steady state electric field distribution. The impact of the ion source external magnetic field in the electron/ion dynamics was not included in the present study.

3.1. Electrostatic field distribution within the anode volume

Fig. 3 shows the contour lines for the electrostatic field distribution (after the quasi-steady state described above has been reached) when applying 100 V to the anode walls (VADIS-mode of operation). Electrons are launched from a circular surface with an initial homogeneous spacial distribution representing the cathode. An electron current of

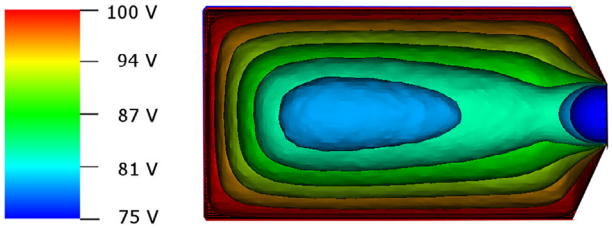

Fig. 3. Simulated electrostatic field distribution inside the anode (exit aperture on the right hand side) with an anode voltage of 100 V (VADIS-mode) and the electron current to 20 mA. Ions created at a location corresponding to an equipotential field line linked to the extraction aperture will be successfully extracted while those created in the potential well (blue region in the center of the source) will be trapped.

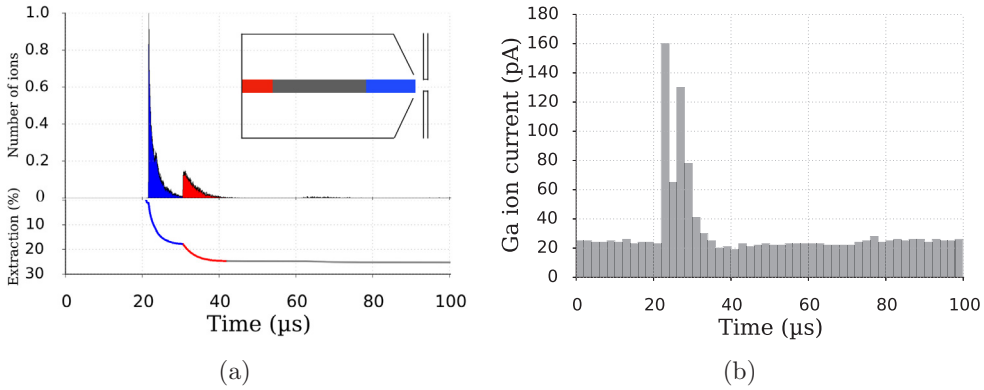

Fig. 4. (a) Simulated time structure of Ga^+ with VSim – extraction plates at 0 V and anode at 20 V (top panel) and integrated number of ions from 0 to 100 μs (time between two laser pulses) normalized to the total number of ions created during one laser pulse (lower panel). The inset represents the ion's origin in the anode volume and the color code is the same as in the figure. (b) Experimental time structure of $^{71}Ga^+$ measured with a Faraday cup at the focal plane of the dipole separator magnet.

20 mA is used as an input parameter for the simulation taking into account that the anode grid transparency is ~50%. This value is comparable with the 40 mA current measured experimentally for a cathode operation temperature of 1935 °C. The results are in broad agreement with earlier studies [8] which used the CPO software [9].

The ion source efficiency depends on the ionization efficiency, ion survival and extraction probability. Since the anode exit aperture is small compared to its internal surface area it is particularly important for the electrostatic field distribution to provide ion confinement (preventing anode wall collisions) and to result in ion flow towards the exit aperture.

The consequence of this, however, is that satisfying this requirement typically results in a region of the potential well in the centre of the anode volume where ions are confined from reaching the anode walls and the exit aperture. They are therefore trapped. This is illustrated in Fig. 3 – where the central blue area corresponds to this trapped region. In [8] the ratio of this trapped region to the active region (ion confinement but with access to anode aperture) was identified as the primary difference between MK5 and MK3 FEBIAD geometries responsible for the different efficiencies of these two ion sources. Based on these considerations, a reduction in the volume of this inactive region will result in an increase in ion source efficiency. In VADIS-mode, ion creation takes place throughout the full anode volume while in RILIS-mode ions are created only where the laser beam is present: a well defined central region in a cylinder with a diameter of 1.5 mm (the exit hole diameter of the VADIS). The initial VADLIS investigations suggested this potential well, which also appears when the ion source is operated in RILIS-mode, resulted in a comparatively slow release of laser-ionized ions from this region [1].

3.2. Laser ionization as a probe to study the electrostatic field distribution and ion extraction time structure

The histogram of the ion arrival time at the detection system, relative to the moment of ion creation (the laser pulse arrival time), provides the time structure of the ion beam generated at the ion source. The field distribution inside the ion source has a strong impact on the time structure of the laser-ionized beam. The time structures from the first VADLIS investigations [1] were qualitatively interpreted as resulting from ionization in three distinct regions along the length of the anode cavity. An analysis of the time structures can provide information about the field distribution, as well as the ion survival and the probability for an ion to be extracted.

To validate and better describe the time structure interpretation given in Ref. [1], a column of uniformly distributed ions is placed in the calculated electrostatic field along the axis of the ion source, representing the ions created in the region of interaction of the laser beam with the atoms. The length of the laser pulse is in the ns range, small compared to the ion motion time scale. Therefore we consider the ions are created instantaneously. Because of the relative low atom density, the number of photo-electrons created by the laser pulse is sufficiently small not to perturb the static electrical field simulated previously. It is therefore assumed in the calculation that ions are subject to this predefined and unchanging electric field distribution. These approach is advantageous given the charge to mass ratio of the electrons is 3–5 orders of magnitude smaller than that of the ions and as a result the ions experience much smaller acceleration due to the same field magnitude. These assumptions are therefore necessary to enable the simulation to run in time steps suitable for ion, rather than electron, motion. Since we do not model explicitly the electron–ion dynamics at the same time, ion–electron neutralization mechanisms were not taken into account.

With the anode voltage set at 20 V in the simulations we study the ion time structure (this voltage value was chosen to study the time profile of the ions created within the anode volume and will be compared to the time structure measured experimentally at this same voltage). The electron current which determines the electrostatic field distribution was set to 1.5 mA since just half of the electrons reach the anode volume due to the 50% grid transparency (3 mA was measured experimentally at 1935 °C though this number was observed to go up to 12 mA for a different ion source). Considering a 1 nA laser-ionized Ga^+ beam with a 1.5 mm diameter (defined by the aperture of the extraction plates) and 23.16 mm length (length of the anode cavity) ion creation cylinder, the ion density along the laser beam path from a single overlapped set of laser pulses is of the order of $10^{11}/cm^3$.

The simulated results show good agreement with the qualitative interpretation given in [1], with the time structure (Fig. 4a (top panel)) showing two distinct peaks. A prompt release peak, appearing after ~21 μs, (corresponding to the time-of-flight of the ions from the source to the Faraday cup) was associated to the ions created by the laser pulse in the region close to the exit-hole aperture and first to feel the extraction field. The second peak of the prompt release, appearing ~10 μs later can be associated to regions where the potential is high enough to overcome the potential well present at the rear of the ion source, which is the case for the ions created near the anode grid (see Fig. 1 and Fig. 3). These statements were validated by tagging each ion inside the ion source according to their horizontal coordinate with a color code and observing how the particles are extracted from the volume as a function time. Fig. 4a (lower panel) shows that up to 18% of the ions are extracted within 10 μs after ion creation and 10 μs later, the percentage of ions extracted from the ion source equals 25%.

According to the simulation, approximately 75% of the ions are not released within 100 μs, but remain confined within the region of enclosed electrical potential (Fig. 4a (lower panel)). In fact, it is demonstrated in Ref. [11] that, by operating the lasers with a 2kHz repetition rate, the laser related ions residency time within the cavity exceeds 500 μs.

To validate these results, the experimental time structure of the extracted beam was obtained through a sliding beam gate technique: by applying a pulsed high voltage source to a vertical deflector plate downstream of the extraction electrode a fast beam gate was realized.

The variable-width beam gate was operated at the repetition rate of the pulsed RILIS lasers (10kHz) and triggered, with adjustable delay from the master clock that triggered the laser.

The Ga^+ signal was recorded while a 10kHz beam gate (gate open) of 2 μs duration was applied. The measurement was repeated for different gate delay times across the 100 μs interval between laser pulses. The results are shown in Fig. 4b. The ions generated within the central (grey) region on Fig. 4a (inset), are not extracted within the time-window between laser pulses, and therefore form a 'DC' background in the experimentally-observed time structure (Fig. 4b). A laser on/off measurement proved that 50% of this DC background current is attributed to laser-ionized Ga. One notices also two distinct time structures on top of the DC background current. We can evaluate the ratio of ions found in the prompt release (from a single laser pulse) to this slow-release DC component to be 1:1.3 (calculated after subtraction of the non laser-ionised DC background). This is in agreement with earlier studies which indicated that the majority of the ions are slowly extracted on a time scale which is long compared to the time between laser pulses [1,11]. The ion survival time in the anode volume is therefore sufficiently long for the ion population to build up, exceeding the capacity of the potential well.

The general features of both the experimental and theoretical time structures are consistent. The two peaks appearing in the experimental time structure, separated by ~4 μs as shown in Fig. 4b is consistent with the existence of a voltage depression. The spacing in time of these peaks as well as their intensity will depend on the electron density in the cavity and anode voltage, since it is the electron density that determines the field distribution and depth of the potential well.

The information provided by the simulated and experimental time structures shown in Fig. 4 enables an estimation of the extraction efficiency of the slow-release component of the laser-ions. From the simulation (Fig. 4a), we see that the prompt release accounts for 25% of the ions generated by one laser pulse. The remaining ions are either not released (trapped or re-neutralised), or released slowly with respect to the 100 μs between laser pulses. Using the assumption that the electrostatic field used for the simulation in Fig. 4a remains unchanged after many laser pulses, and that the ion-survival for the ions originating in the prompt release regions (colored regions in Fig. 4a (inset)) is 100%, the extraction efficiency for the ions generated in the 'trapped' region is estimated to be 42%, resulting in an overall ion extraction efficiency of 57%. As will be shown in Section 4.3, even with an anode voltage of 20 V, the application of an optimal voltage to the extraction plates (see Fig. 1) results in an enhancement in overall efficiency of ~30%.

4. VADLIS with improved extraction characteristics of laser-ions

The electrical field distribution inside the anode due to the potential difference between the anode body and the locally grounded extraction plates, has an effect on the ion extraction. Here we investigate the recovery of an effective potential difference, that can be optimized for maximum ion extraction probability while operating in RILIS-mode. This can be achieved by applying a negative voltage to the extraction plates aperture of the ion source. The present study was performed using the VSim software, leading to the construction of a VADLIS prototype that presents improved ion extraction characteristics as demonstrated experimentally.

4.1. Dependence of electrical field distribution on the extractor-plate voltage

A comparison between the field distribution inside the anode cavity of the VADIS when the extraction plates are set to 0 V and −100 V is shown in Fig. 5. For both cases, the anode voltage is set to 1.35 V and the electron drain current (the electron current from the cathode to the anode) to 0.2 mA, corresponding to the value measured during optimal RILIS-mode operation. At such low voltages no significant electron impact ionization takes place (1.35 eV is below the threshold for electron impact ionization of Ga). As shown in Fig. 5a, an electrical potential well of ~1 V depth with respect to the anode walls is established towards the rear of the source. This means that ions created in this region will not be extracted (or the extraction will be slow since it will require the accumulation of enough ions to exceed the capacity of this potential depression) since their thermal energy is insufficient to overcome this potential well.

Biasing the voltage of the extraction plates to −100 V (Fig. 5b) results in an extraction field which penetrates deeper into the anode volume to better satisfy the efficiency requirements discussed earlier: ion confinement to prevent wall collisions, a field distribution that results in ion flow towards the exit aperture, and a reduction of ion trapping effect in the 'inactive' anode space.

Fig. 6a represents the potential along the axis of the anode cavity. Only the positive voltage values are displayed, however the curves corresponding to the extraction voltages of 0 V and −100 V reach a value of −6 V and −39 V at the anode exit respectively.

The solid curve in Fig. 6a represents the simulated potential along the axis of the ion source when the extraction plates are at 0 V. Ions created in the light grey regions shown in Fig. 6a will be extracted. This is due to the fact that their initial positions lie outside the potential barrier defined by the solid vertical lines (trapping region). In the same way, when applying −100 V to the extraction plates, this trapping region is reduced (defined by the vertical dashed lines). As a result, the volume of the region from which ions can be successfully extracted increases and is represented by the dark grey area in Fig. 6a.

The percentage of ions extracted within the first 100 μs can be related to the length along the x-axis defined by the shaded regions shown in Fig. 6a. This is because the laser-ions are assumed to be created and uniformly distributed in a cylinder of laser illumination along the axis of the ion source. For 0 V, this percentage equals 32% and increases to 48% for −100 V applied to the extraction plates.

The percentage of ions remaining within the ion source as a function of time is represented in Fig. 6b for 0 V (Fig. 5a) and −100 V (Fig. 5b) respectively. It shows a faster and more efficient extraction of the ions when the extraction plates are biased to −100 V. The extraction efficiency within the first 100 μs is calculated to improve from 32% to 48%, in agreement with the evaluation from Fig. 6a. After many laser pulses and accumulation of ions in the potential well region, ions will be able to escape more easily when −100 V are set in the extraction plates due to a shallower potential well compared to the standard configuration. It can also be noticed that when comparing Fig. 6b and Fig. 4a (lower panel), the extraction efficiency of the prompt release it is higher for the case of 1.35 V applied to the anode walls (32%) compared to when the voltage of the anode is 20 V (25%). For 20 V more electrons are drawn from the cathode, which results in a higher electron density and deeper potential well.

The ions created near the exit aperture will suffer from a larger energy spread. Considering an energy spread that the ISOLDE mass separators can accept of 20 eV, only ions created at a position within the ion source higher than 22.4 mm will not be transmitted through a slit corresponding to the standard resolving power of the mass separator. This means that for the case in which the extraction plates are set to −100 V, the relative fraction of ions with an energy spread larger than 20 eV is only of 3% of the total extracted beam.

The increase in energy spread of the extracted ions when applying a voltage of −200 V on the extraction plates was also visible in the experimentally measured mass spectra. The mass resolution M/ΔM for ^{71}Ga decreased from 1200 (at 0 V) to 600 (at −200 V).

4.2. Adjustable-extractor VADLIS prototype

In order to validate the improved ion extraction suggested by the aforementioned simulations, a VADIS with an adjustable-voltage extraction plate has been constructed and tested at the ISOLDE off-line

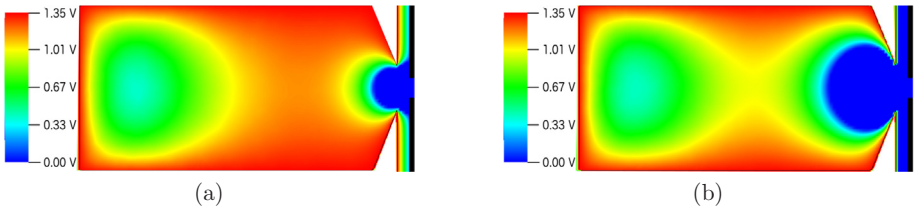

Fig. 5. Electrostatic field distribution simulated with VSim with anode walls at 1.35 V (optimal value for RILIS-mode efficiency) and 0.2 mA electron current: (a) 0 V extraction plates; (b) −100 V extraction plates. The color scale is adjusted to best visually depict the [0 V, 1.35 V] region. Values at 0 V and below appear as dark blue. The consequences in terms of energy spread of the ions generated in this region are discussed in the text.

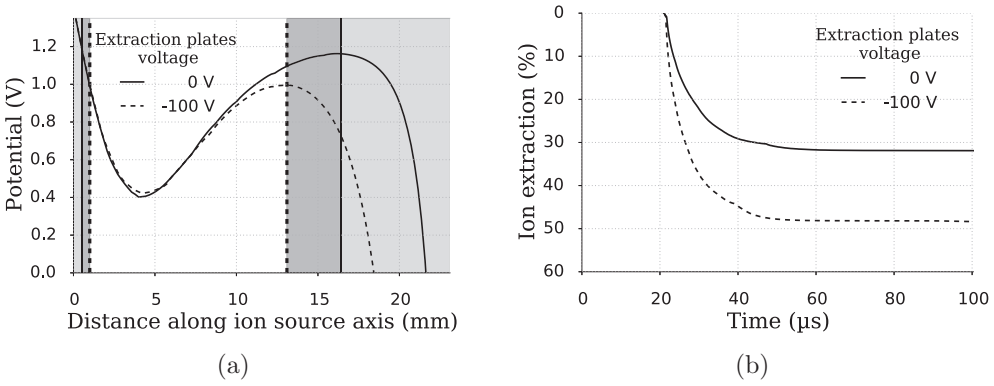

Fig. 6. (a) Potential along the axis of the anode cavity for 0 V (solid line) and −100 V (dashed line) set on the extraction plates. The x-axis represents the full length of the anode cavity (23.1 mm). The y-axis shows the potential within the source just in the range [0 V, 1.35 V] b) Percentage of ions extracted from the anode volume as a function of time. Details about the meaning of the shadowed areas are given in the text.

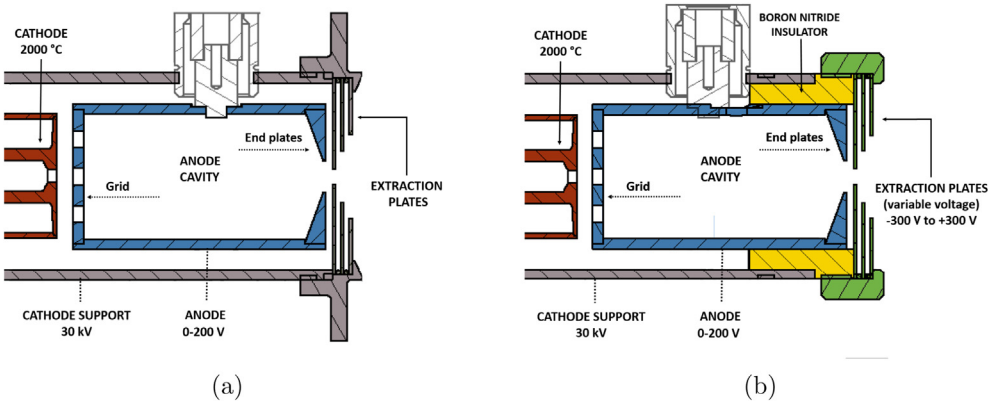

Fig. 7. (a) Standard VADIS used at ISOLDE based on the MK5 FEBIAD geometry (just one out of three anode holders shown); (b) VADIS with BN insulator. In this case just one anode holder was used to allow the electrical connection of the anode. Extraction plates can be biased with a voltage in the range from −300 to +300 V.

laboratory. The differences between the standard VADIS and the new version are highlighted in Fig. 7b. The extraction plates are mounted in a boron nitride (BN) cylinder, leaving them insulated from the target unit and allowing the application of an independent voltage.

This modification has the additional advantage of improving the structural stability of the ion source: the anode cylinder is screwed into the BN insulator, rather than being held by three insulating screws as can be seen in Fig. 7a. The relevant distances for the standard performance of the source when operated both on-line and off-line were kept the same (cathode-grid distance = 1.5 mm, extraction plate aperture diameter = 1.5 mm). The source was operated for a period of more than a month in which multiple cycles of cooling and heating were performed demonstrating its reliability and showing the new BN component withstands thermal expansion of the metal parts.

The new configuration showed typical ion source performance under standard operation conditions. The $^{84}Kr^{+}$ ion current produced by electron impact ionization in the VADIS operation mode was monitored during the whole period of operation. The obtained total efficiency remained between 16 and 25% at the cathode temperature of 2030 °C when operated at 100 V anode voltage, which is comparable to typically measured values with a standard VADIS unit. This is a typically used reference parameter at ISOLDE for testing the VADIS ion source performance.

4.3. Experimental results using the adjustable-extractor VADLIS prototype

The performance of the new VADLIS source was investigated by measuring the intensity of $^{71}Ga^{+}$ ion beam produced in the RILIS-mode under different combinations of the anode voltage (V_a) and the extraction plates voltage (V_e). The obtained results are presented in Fig. 8 and Table 1.

Fig. 8a shows the $^{71}Ga^{+}$ beam intensity for the extractor voltage range V_e [0, −140 V] and an anode voltage range V_a [0, 2 V] (falling within region I in Fig. 2). Fig. 8b shows the same in the ranges V_e [0, −60 V] and V_a[10, 25 V] (corresponding to region II in Fig. 2). At V_e = 0 V, corresponding to the standard VADIS configuration, the maximum current measured in the range V_a [0, 2 V] is 113 pA at 1.35 V and decreases as the anode voltage increases. The decrease in laser-ionized Ga^{+} current for V_a > 1.35 V is due to the anode voltage exceeding the voltage drop of the resistively heated cathode. Ga^{+} ions originating from the cathode tube are therefore suppressed since they are unable to pass the anode grid to enter the anode volume.

For V_a < 1.35 V, the ion current is less sensitive to changes in the voltage of the extraction plates compared to V_a > 1.35 V as can be observed in Fig. 8a. When V_a < 1.35 V, the ions created by the laser light inside the cathode flow towards the anode cavity due to the voltage gradient that exists inside the cathode. These ions can be

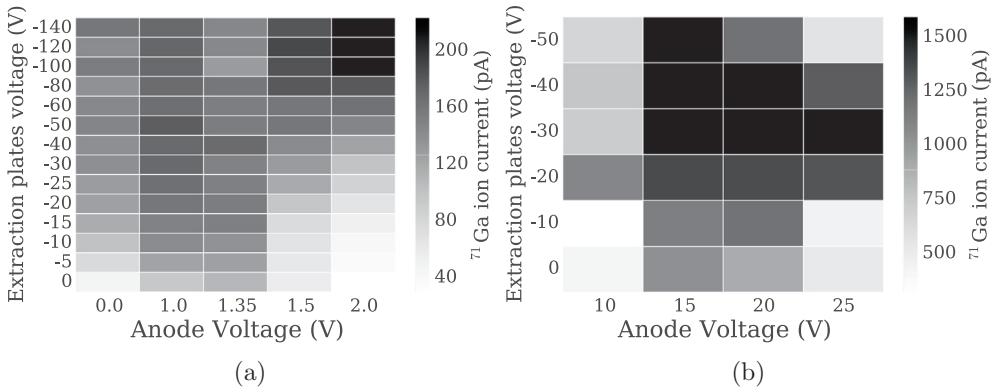

Fig. 8. Voltage scan of V_a and V_e for (a) region I and (b) region II as defined in Fig. 2. Note: the data represented in Fig. 8a and Fig. 8b were taken during different measurement periods and consistency in terms of all experimental conditions (laser alignment, power, ion beam purity, electron emission etc) could not be guaranteed. Therefore, the intensity ratios observed when going from region I to region II do not correspond to the ion signal ratios observed in the anode scan shown in 2.

Table 1
Experimentally measured ion rates for different anode voltages with and without the application of the extractor plate voltage for region I. Here $V_{e.opt}$ refers to the value of V_e for which the ion signal is the highest.

V_a (V)	I [V_e = 0 V] (pA)	I [$V_{e.opt}$] (pA)	$V_{e.opt}$ (V)
0.0	50	170	−140
1.0	100	187	−50
1.35	113	179	−40
1.5	60	200	−120
2.0	30	223	−120

Table 2
Enhancement factor obtained when optimizing the extraction plates voltage for maximum ion extraction in RILIS-mode. The anode voltage V_a and the source magnet current were optimized in each case for maximum ion extraction efficiency.

Isotope	Background V_e = 0 V	Lasers On V_e = 0 V	Lasers On(*) $V_{e.opt}$	Enhancement factor	Laser scheme (nm)) $\{\lambda_1|\lambda_2|\lambda_3\}$
^{24}Mg	8 pA	8.5 nA	23.5 nA	2.8	{285|553|532} [17]
^{98}Mo	0 pA	13.4 pA	103 pA	7.7	{380|416|635} [21]
^{196}Hg	18 pA	58 pA	133 pA	2.3	{256|313|532} [22]

(*) The Lasers Off signal for $V_{e.opt}$ is also expected to increase, however this value was not measured.

successfully extracted once they traverse the anode grid. All ions passing the anode grid enter the active region of the anode volume and are therefore rapidly and efficiently extracted.

With $V_a > 1.35$ V (within the region represented in Fig. 8a), most of the observed Ga^+ ions are generated inside the anode volume rather than in the hot cathode. Since these ions have a point of origin that is not necessarily in the active region of the anode, a higher proportion of these ions have an extraction probability that is dependent upon the extraction aperture voltage V_e.

The maximum Ga^+ signal when $V_e = 0$ V equals 113pA (for $V_a = 1.35$ V), see Table 1. When tuning the voltage of the extraction plates to maximize the extracted Ga^+ beam current, a value of 223pA was achieved. These results demonstrate that, by having an independently-adjustable extractor plate voltage, the ion extraction efficiency of the VADLIS in RILIS-mode can be improved by a factor 2. In a similar way for region II, a 30% increase in the Ga^+ signal was observed. Operating the ion source in this region has the advantage of suppressing the incoming ions from the cathode. This is desirable if the required beam suffers from surface-ionized isobaric contamination.

In November 2017 the first on-line test of the modified VADLIS was performed at ISOLDE. The target material was a magnesium oxide (MgO − 9.8 g) and uranium oxide (UO_2 − 92.2 g) mixture, specifically chosen for the production of molecular beams for a separate beam-development activity. Magnesium and molybdenum atoms were available from the target-ion source assembly, with magnesium evaporating from the target material and molybdenum from the anode grid, whilst mercury was either radiogenically produced or present as a contaminant in the target material. The target was operated in the range of 780 to 1200 °C while the cathode of the ion source was kept at ~2000 °C. The enhancement in the magnesium, molybdenum, and mercury laser-ion signal when optimizing V_e for maximum ion extraction in the RILIS-mode of operation is shown in Table 2. The optimal anode voltages V_a for ^{24}Mg,^{98}Mo and ^{196}Hg were 1, 0 and 1 V respectively.

In our tests magnesium, mercury and gallium reach the anode by travelling along the cathode tube. In contrast, the anode body itself is the source of the molybdenum atoms. This difference is reflected in the enhancement factor achieved when optimizing the extraction voltage V_e for Mg, Hg and Ga (2 to 3), compared to Mo (7.7). This is as expected, since ions originating outside of the anode volume (Mg, Ga, Hg) enter the anode through the grid and therefore have enough kinetic energy to reach the extraction aperture as shown in Fig. 6a. Their extraction probability is therefore independent of the extraction voltage settings. The situation for Mo (factor 7.7 enhancement) is analogous to that of ^{71}Ga depicted in the right-hand column in Fig. 8a, when the anode voltage ($V_a = 2$) is sufficient to suppress the cathode ions. At this point, the enhancement factor achieved by optimizing the extractor voltage becomes 7.3.

The VADIS efficiency for Ga, Mg and Hg have been measured at the off-line laboratory in a separate set of measurements to be 12%, 6% and 9% respectively [23]. Assuming an equal VADIS-mode and RILIS-mode efficiency (as is typically shown in the laser-on anode scans), the RILIS-mode efficiency of the VADIS with optimally biased extraction plates is expected to be 24% (Ga), 12% (Mg) and 18% (Hg).

5. Conclusions and outlook

Previous studies have demonstrated that the anode cavity of the VADIS ion source serves as an efficient laser-atom interaction region. We used the VSim particle-in-cell software to study the electrostatic field distribution inside the anode cavity and the ion time structure. The general features observed in the calculated time structure with the help of VSim simulation code matched the experimentally measured values and the interpretations of previous work.

The simulated electrostatic field distribution within the anode

volume of the VADLIS when operating in RILIS-mode was compared to a simulation of a cavity with better laser-ion extraction characteristics. The simulations showed an increase in the active region of the latter, favourable for the extraction of laser-ions created in the anode volume within the first 100 μs of ionization when biasing the voltage of the extraction plates to negative values, which gives the flexibility of optimizing the extraction field for maximum ion extraction probability.

Based on the input of the simulations, a new prototype ion source was designed. During off-line tests of the prototypes, no loss of reliability was observed. On the contrary, the insulator design enables a more structurally-sound means of securing the anode chamber, and potentially eliminates some VADIS failure modes such as short circuit caused by tilting of the anode chamber. A twofold increase in efficiency was observed in RILIS-mode with this prototype for gallium during the off-line testing period. This modified VADLIS was also operated on-line at the ISOLDE facility showing an enhancement factor greater than 2 for the stable isotopes tested (^{24}Mg, ^{98}Mo and ^{196}Hg). The extraction voltage V_e allows for the operation of the ion source in a regime for which surface ions created inside the cathode tube are suppressed while an enhancement in overall signal can still be achieved.

The agreement between the experimental and simulated results obtained so far indicate that VSim can be used to optimize the anode cavity geometry for improved RILIS and VADIS mode performance. Following the validation of this approach to optimizing ISOLDE ion sources, we will aim to continue this work to find the optimal RILIS-mode VADLIS geometry and design. Re-purposing the anode grid, and decoupling its polarization from the anode body, offers an additional parameter which can be used to change the electron energy and electron flux. This would enable a switching from RILIS-mode to VADIS-mode without changing the extracted beam energy. This is important for maintaining optimal conditions for energy-sensitive beam manipulations downstream (such as for injection in the REXTRAP/EBIS [24,25]). Such modification allows better diagnostics of the ion source, enabling the measurement of the electron drain current at different anode components (grid, body, extractor).

The modified VADLIS ion source has been shown to be reliable and highly versatile, while offering an improved efficiency compared to the standard VADLIS. These characteristics are expected to be particularly important for next-generation ISOL facilities (SPES [26], SPIRAL2 [27], ISOL@MYRRHA [28]) where the target lifecycle is expected to be long (weeks-months), or for cases where a wide variety of species will need to be extracted from a single target-ion source assembly (e.g. CERN-MEDICIS [29]). Regular target/ion source changes to suit specific experiments are therefore less practical.

This work represents an important step forward in the development and exploitation of the VADLIS as the most versatile ion source for ISOL facilities. We propose this could be a favourable standard configuration for operation at ISOLDE. It would offer unmatched versatility combined with the option of high selectivity, without compromising standard VADIS performance and reliability.

Acknowledgements

This work has been funded by FWO-Vlaanderen (Belgium), by GOA/ 2010/ 010 (BOF KU Leuven), by the IAP Programme initiated by the Belgian Science Policy Office (BriX network P7/12), by the European Commission within the European Nuclear Science and Application Research ENSAR2 (Grant agreement No. 654002) and by a Grant from the European Research Council (ERC-2011- AdG-291561-HELIOS). The authors would like to thank the support received from the European Union's Horizon 2020 research and innovation programme under grant agreement No. 642889 MEDICIS-PROMED.

References

[1] T. Day Goodacre, J. Billowes, R. Catherall, T.E. Cocolios, B. Crepieux, D.V. Fedorov, V.N. Fedosseev, L.P. Gaffney, T. Giles, A. Gottberg, K.M. Lynch, B.A. Marsh, T.M. Mendonça, J.P. Ramos, R.E. Rossel, S. Rothe, S. Sels, C. Sotty, T. Stora, C. Van Beveren, M. Veinhard, Blurring the boundaries between ion sources: the application of the RILIS inside a FEBIAD type ion source at ISOLDE, Nucl. Instrum. Methods Phys. Res., Sect. B: Beam Interact. Mater. At. 376 (2015) 39–45.
[2] R. Kirchner, E. Roeckl, A novel ISOL ion source, Nucl. Instrum. Methods 139 (1976) 291–296.
[3] V.N. Fedosseev, Yu. Kudryavtsev, V.I. Mishin, Resonance laser ionization of atoms for nuclear physics, Phys. Scr. 85 (5) (2012) 058104.
[4] L. Penescu, R. Catherall, J. Lettry, T. Stora, Development of high efficiency Versatile Arc Discharge Ion Source at CERN ISOLDE, Rev. Sci. Instrum. 81 (2) (2010) 1–5.
[5] R. Catherall, W. Andreazza, M. Breitenfeldt, A. Dorsival, G.J. Focker, T.P. Gharsa, T.J. Giles, J.-L. Grenard, F. Locci, P. Martins, S. Marzari, J. Schipper, A. Shornikov, T. Stora, The ISOLDE facility, J. Phys. G: Nucl. Part. Phys. 44 (9) (2017) 094002.
[6] S. Sundell, H. Ravn, Ion source with combined cathode and transfer line heating, Nucl. Instrum. Methods Phys. Res., B 70 (1–4) (1992) 160–164.
[7] C.D. Child, Discharge from hot CaO, Phys. Rev. (Series I) 32 (5) (1911) 492–511.
[8] L. Penescu, Techniques to Produce and Accelerate Radioactive Ion Beams (Ph.D. thesis), Polytechnic Inst., Bucharest, 2009 https://cds.cern.ch/record/2259078?ln=en.
[9] CPO programswww.electronoptics.com.
[10] L. Penescu, R. Catherall, J. Lettry, T. Stora, Numerical simulations of space charge effects and plasma dynamics for FEBIAD ion sources, Nucl. Instrum. Methods Phys. Res., Sect. B 266 (19–20) (2008) 4415–4419.
[11] T. Day Goodacre, Developments of the ISOLDE RILIS for Radioactive Ion Beam Production and the Results of their Application in the Study of Exotic Mercury Isotopes (Ph.D. thesis), The University of Manchester, 2016 https://cds.cern.ch/record/2254839.
[12] D. Lunney, Extending and refining the nuclear mass surface with ISOLTRAP, J. Phys. G: Nucl. Part. Phys. 44 (6) (2017) 064008.
[13] M. Breitenfeldt, D. Atanasov, K. Blaum, T. Eronen, P. Finlay, F. Herfurth, M. Kowalska, S. Kreim, Yu. Litvinov, D. Lunney, V. Manea, D. Neidherr, T. Porobic, M. Rosenbusch, L. Schweikhard, N. Severijns, F. Wienholtz, R.N. Wolf, K. Zuber, Q-values of Mirror Transitions for fundamental interaction studies. CERN INTC proposal P-369, 2013.
[14] J. Karthein, Precision mass Measurements using the Phase-Imaging Ion-Cyclotron-Resonance Detection Technique (Master thesis), University of Heidelberg, 2017 https://cds.cern.ch/record/2300223?ln=en.
[15] C. Nieter, J.R. Cary, VORPAL: a versatile plasma simulation code, J. Comput. Phys. 196 (2) (2004) 448–473.
[16] VSimhttps://www.txcorp.com.
[17] V.N. Fedosseev, L.E. Berg, D.V. Fedorov, D. Fink, O.J. Launila, R. Losito, B.A. Marsh, R.E. Rossel, S. Rothe, M.D. Seliverstov, A.M. Sjödin, K.D.A. Wendt, Upgrade of the resonance ionization laser ion source at ISOLDE on-line isotope separation facility: new lasers and new ion beams, Rev. Sci. Instrum. 83 (2) (2012) 02A903.
[18] R. Kirchner, On the thermoionization in hot cavities, Nucl. Instrum. Methods Phys. Res., Sect. A 292 (2) (1990) 203–208.
[19] V.I. Mishin, V.N. Fedoseyev, H.-J. Kluge, V.S. Letokhov, H.L. Ravn, F. Scheerer, Y. Shirakabe, S. Sundell, O. Tengblad, Chemically selective laser ion-source for the CERN-ISOLDE on-line mass separator facility, Nucl. Instrum. Methods Phys. Res., Sect. B 73 (4) (1993) 550–560.
[20] J. Lettry, R. Catherall, U. Köster, U. Georg, O. Jonsson, S. Marzari, V. Fedosseev, Alkali suppression within laser ion-source cavities and time structure of the laser ionized ion-bunches, Nucl. Instrum. Methods Phys. Res., Sect. B 204 (2003) 363–367.
[21] RILIS Databasehttp://riliselements.web.cern.ch/riliselements/.
[22] T. Day Goodacre, J. Billowes, K. Chrysalidis, D.V. Fedorov, V.N. Fedosseev, B.A. Marsh, P.L. Molkanov, R.E. Rossel, S. Rothe, C. Seiffert, K.D.A. Wendt, RILIS-ionized mercury and tellurium beams at ISOLDE CERN, Hyperfine Interact. 238 (1) (2017) 41.
[23] Y. Martinez Palenzuela, (Ph.D. Thesis). KU Leuven. In preparation.
[24] B.H. Wolf, J. Cederkäll, O. Forstner, F. Wenander, F. Ames, K. Reisinger, L. Liljeby, Ö. Skeppstedt, B. Jonson, G. Nyman, First radioactive ions charge bred in REXEBIS at the REX-ISOLDE accelerator, Nucl. Instrum. Methods Phys. Res., Sect. B: Beam Interact. Mater. At. 204 (2003) 428–432.
[25] P. Schmidt, F. Ames, G. Bollen, O. Forstner, G. Huber, M. Oinonen, J. Zimmer, Bunching and cooling of radioactive ions with REXTRAP, Nucl. Phys. A 701 (1–4) (2002) 550–556.
[26] G. de Angelis, G. Fiorentini, The Legnaro National Laboratories and the SPES facility: nuclear structure and reactions today and tomorrow, Phys. Scr. 91 (11) (2016) 113001.
[27] M. Lewitowicz, The SPIRAL2 Project and experiments with high-intensity rare isotope beams, J. Phys: Conf. Ser. 312 (5) (2011) 052014.
[28] L. Popescu, Nuclear-physics applications of MYRRHA, EPJ Web Conf. 66 (2014) 10011.
[29] R.S. Augusto, L. Buehler, Z. Lawson, S. Marzari, M. Stachura, T. Stora, the CERN-MEDICIS Collaboration, CERN-MEDICIS (Medical Isotopes Collected from ISOLDE): a new facility, Appl. Sci. 4 (2) (2014) 265–281.